

Dynamics of quadrature-variance in high-harmonics generation

Ákos Gombkötő¹

¹*Department of Theoretical Physics, University of Szeged, Tisza Lajos körút 84, H-6720 Szeged, Hungary*

We analyse the quadrature variance, or (anti-)squeezing properties of the high harmonic photons. We use a simplified model associated with High-harmonic generation (HHG) in the case of an elementary quantum source, modelled with a two-level atom [1]. Assuming classical excitation, we find weak, oscillating (anti-)squeezing in the scattered radiation, with the squeezing spectrum following similar evolution to the photon-number spectrum. Investigating the phase-relations, we conclude that the squeezed states of each mode are –most of the time– close to being amplitude-squeezed, and squeezed states appear practically periodically within each attosecond pulse. We have also defined an approximate single noise-ellipse based on the collective field, and its analysis shows that it is anti-squeezed.

PACS numbers:

I. INTRODUCTION

Attosecond pulses push the limits of high-precision measurement to unprecedented scales. Historically attosecond science have been largely described semi-classically, treating the electron quantum-mechanically, and the electromagnetic field classically [2–4]. This description naturally can not capture all characteristics of the process. In order to capture or control ultrafast processes by using sequences of few-cycle optical pulses, a proper characterization is necessary, both in amplitude and phase.

Generation of attosecond pulses is made possible mainly by high harmonic generation (HHG) containing many possible experimental realisations. HHG is a strongly nonlinear optical effect that plays central role in attosecond physics [3, 5, 6]. The sufficient degree of control however, has not yet been achieved for few-cycle pulses generated by high-order harmonic generation.

In the characterization of short pulses, until the advent of femtosecond techniques, the carrier-envelope phase was of little practical interest. On the other hand it is an important quantity in attosecond science. The measurement of the carrier-envelope phase of a single attosecond pulse has been discussed theoretically in a semiclassical frame before [7], and experimentally demonstrated by probing intraband currents [8]. Relative phases between consecutive attosecond pulses has been investigated both theoretically and experimentally in [9]. However, direct measurement of phase-quantities in attosecond pulses so far has not been feasible in a reliable way.

While a strong, coherent pulse may indeed have well-defined amplitude and phase, if the short pulse has low intensity, the classical pictures associated with it becomes less practical, and the concept of carrier-envelope phase is no longer applicable due to the excessive phase uncertainty. We note that while generation of pulses with 200as length, and $10^{18}\text{W}/\text{cm}^2$ peak intensity has been reported [10], this is far from being typical.

It has been argued [11] that for weak pulses, instead

of the phase, relative timing of a quantum noise pattern gains relevance. Stemming from this idea, we focus our attention to the time-dependent squeezing properties associated with attosecond pulses.

At the same time, squeezed light is a historically important phenomena in quantum optics, and not only fundamental, but also applied science have benefitted a lot from using squeezed light, being a valuable tool of metrology and for quantum information processing. Both the degree of squeezing and the squeezing bandwidth are important for potential applications. Current experiments with pulsed squeezed light reach a bandwidth up to tens of THz [12]. Sub shot-noise measurements in spectroscopy, sub-wavelength image discerning and recording are just a few examples [13–15]. It has also been proposed that strong intensity fluctuations can enhance multi-photon processes compared to classical light of the same intensity [16]. Significant increase in lateral displacement measurement has been demonstrated in [17], using squeezed beams. Optical solitons of few hundred femtosecond length, and significant squeezing has been achieved [18, 19], and recently it has become possible to generate and analyse time-locked patterns of quadrature squeezed noise, through sampling with femtosecond pulses in a non-destructive manner [20].

Generation of pulsed broadband ultrashort squeezing can be analyzed either in the traditional approach of quantum optics, quantizing single-frequency modes [21], or within the time-domain frame [11, 20]. While the latter, novel approach is in many respect better fitted to model short pulses, there are (as of current) certain limitation in it; such as the neglect of dispersions. Since in the high-harmonic generation absorption plays role, we will not follow this route.

II. MODEL

In our model, we will assume that the femtosecond pulses are –at least before interaction– characterized by coherent states. The assumption that the interaction of

the pulse with matter only perturbs the quantum statistics has been investigated independently in [22]. The intensities of the generated harmonics are by orders of magnitude lower than the excitation, therefore we will consider quantized harmonic modes.

The model of the material is a two-level system, which may be an acceptably used to describe harmonic generation in semiconductor heterostructures [23]. On the other hand, the simplicity of two-level systems help forming qualitatively (and often quantitatively) correct predictions, and offer insight into the dynamics of the HHG. Furthermore, the methods used in this article can be easily generalized to more complex high harmonic sources as well.

Let us consider the following terms:

$$H_a = \hbar \frac{\omega_0}{2} \sigma_z, \quad H_m = \sum_n \hbar \omega_n a_n^\dagger a_n, \quad (1)$$

$$H_{am} = \sum_n \hbar \frac{\Omega_n}{2} \sigma_x (a_n + a_n^\dagger), \quad (2)$$

where the first term corresponds to the two-level atom, the second term to the quantized electromagnetic modes, and the quantized dipole-interaction corresponds to the third. When the electromagnetic field of the strong exciting pulse can be described classically, then:

$$H_{ex}(t) = -DE(t) = -d\sigma_x E(t) = -\hbar \frac{\Omega(t)}{2} \sigma_x. \quad (3)$$

We note that $\Omega_n = 2d\sqrt{\frac{\hbar\omega_n}{\epsilon_0 V}}$, where V is the quantization volume. Let us denote the eigenstates of the atomic Hamiltonian by $|e\rangle$ and $|g\rangle$, i.e., $H_a|e\rangle = \hbar\omega_0/2|e\rangle$, $H_a|g\rangle = -\hbar\omega_0/2|g\rangle$. We will also use $|+\rangle$ and $|-\rangle$, for which $\sigma_x|\pm\rangle = \pm|\pm\rangle$.

We will consider the laser pulse to be a classical time-dependent excitation. Utilizing the dipole-approximation we are led to the following system [1]:

$$H(t) = H_a + H_m + H_{am} + H_{ex}(t). \quad (4)$$

We will not incorporate spatial functions into our model, and leave out propagation effects.

That a strong classical excitation can drive even at the dipole-approximation a type of nonlinearity that is associated with squeezing, can be seen in Appendix B.

III. MEASURE OF SQUEEZING

In the literature, the term squeezing can be used in different ways. In this article from this point on, we will reserve squeezing to mean only quadrature-squeezing, and will not bother with polarization-; or with higher-order

squeezing [24].

We use the following notations:

$$X_n = \frac{a_n^\dagger + a_n}{2}, \quad Y_n = i \frac{a_n^\dagger - a_n}{2}$$

$$X_{2n} = \frac{a_n^{\dagger 2} + a_n^2}{2}, \quad Y_{2n} = i \frac{a_n^{\dagger 2} - a_n^2}{2}$$

Squeezed states are characterized by canonical observables, in quantum optics typically electric field strength at a given θ phase. The corresponding dimensionless X_n^θ and Y_n^θ operators are defined as:

$$X_n^\theta = \frac{a_n + a_n^\dagger}{2} \cos \theta + i \frac{a_n^\dagger - a_n}{2} \sin \theta,$$

$$Y_n^\theta = -\frac{a_n + a_n^\dagger}{2} \sin \theta + i \frac{a_n^\dagger - a_n}{2} \cos \theta,$$

and for the sake of completeness, we write out the quadratic variances as:

$$\begin{aligned} \langle (\Delta X^\theta)^2 \rangle &= \frac{1}{4} \left(1 + 2\langle N \rangle + 2\langle X_2 \rangle - 4\langle X \rangle^2 \right) \cos^2 \theta \\ &\quad + \frac{1}{4} \left(1 + 2\langle N \rangle - 2\langle X_2 \rangle - 4\langle Y \rangle^2 \right) \sin^2 \theta \\ &\quad + \left(\langle Y_2 \rangle - 2\langle Y \rangle \langle X \rangle \right) \cos \theta \sin \theta, \\ \langle (\Delta Y^\theta)^2 \rangle &= \frac{1}{4} \left(1 + 2\langle N \rangle + 2\langle X_2 \rangle - 4\langle X \rangle^2 \right) \sin^2 \theta \\ &\quad + \frac{1}{4} \left(1 + 2\langle N \rangle - 2\langle X_2 \rangle - 4\langle Y \rangle^2 \right) \cos^2 \theta \\ &\quad - \left(\langle Y_2 \rangle - 2\langle Y \rangle \langle X \rangle \right) \cos \theta \sin \theta. \end{aligned}$$

Quadrature amplitudes are measured in very good approximation with balanced homodyne detectors. Measurements are performed, as usual, on an ensemble of identical states, and quasi-probability density functions are calculated from the data.

Light is called squeezed, if there exists a mode n and phase θ such that $\Delta X_n^\theta < \frac{1}{2}$. However quantification of squeeze is not completely straightforward. The simplest and most widely used method is to measure squeezing for each electromagnetic mode separately:

$$r_n^{(1)} = -10 \log_{10} [4 \min(\Delta X_n^\theta)^2]$$

Further, one can define the spectrum of squeezing [25, 26]. The minimal value is the smaller eigenvalue; and the corresponding phase can be calculated by the associated eigenvector -of the noise-ellipse matrix:

$$\begin{pmatrix} \langle (\Delta X)^2 \rangle & \frac{1}{2} \langle \{\Delta X, \Delta Y\} \rangle \\ \frac{1}{2} \langle \{\Delta X, \Delta Y\} \rangle & \langle (\Delta Y)^2 \rangle \end{pmatrix} \quad (5)$$

The eigenvalues [27] and eigenvectors [28], expressed with

our notations are:

$$\begin{aligned} \lambda_{\pm} &= \frac{1}{4} \left[\langle \{\Delta a, \Delta a^{\dagger}\} \rangle \pm 2|\langle (\Delta a)^2 \rangle| \right] \\ &= \frac{1}{4} \left[1 + 2(\langle N \rangle - \langle X \rangle^2 - \langle Y \rangle^2) \pm 2|\langle X_2 + iY_2 \rangle - \langle X + iY \rangle^2| \right], \end{aligned} \quad (6)$$

and $\begin{pmatrix} u_1 \\ u_2 \end{pmatrix}$ with the components fulfilling:

$$\begin{aligned} (u_{\pm})_1^2 &= \frac{(\lambda^{\pm} - \langle 2X_2 + 2N + 1 \rangle - 4\langle Y \rangle^2)^2}{(\lambda^{\pm} - \langle 2X_2 + 2N + 1 \rangle - 4\langle Y \rangle^2)^2 + \langle 2Y_2 - 4\langle X \rangle \langle Y \rangle \rangle^2} \\ (u_{\pm})_2^2 &= \frac{\langle 2Y_2 - 4\langle X \rangle \langle Y \rangle \rangle^2}{(\lambda_{\pm} - \langle 2X_2 + 2N + 1 \rangle - 4\langle Y \rangle^2)^2 + \langle 2Y_2 - 4\langle X \rangle \langle Y \rangle \rangle^2}. \end{aligned} \quad (7)$$

However, whenever the electromagnetic field in question is multimode, the problem of quantifying squeeze in a few variable is a much more involved problem. It is typically accepted that such fields are to be considered squeezed, if at least one mode is squeezed. Most approach consider discrete n -mode fields, and define a generalized coherence-matrix of $2n \times 2n$ size. After the calculation of eigenvalues, either the lowest eigenvalue, or the product of $\lambda < \frac{1}{4}$ eigenvalues may be used [29]. Other possibilities also exist, such as using Wehrl's entropy [30].

A. On experimental considerations

To date, most balanced homodyne detection measurements have been performed in the frequency domain, where in practice any measurement of the field integrates over some sideband spectrum. A light field is often analysed with respect to many different modulation frequencies, and the result constitutes a spectrum, [31] where in principle every modulation mode can be in a different quantum state. We note that standard homodyne detection suffers from significant bandwidth limitation: While the bandwidth of optical states can easily span many THz, homodyne detection is inherently limited to the electrically accessible, MHz to GHz range, leaving a significant gap between the relevant optical phenomena and the measurement capability. This can be lifted by using parallel homodyne measurement [32].

We note in passing some recent development: It is possible to produce a spectrum of modulation modes that all have the same squeeze angle [33], while introduction of a frequency-dependent squeeze angle was suggested in [34] for gravitational wave detection. It was shown that the optimal frequency dependence that leads to the broadband improvement can be realized by using filter cavities. Motivated by this result, research and development on filter cavities for optimizing the frequency dependence of broadband squeezed fields has been active in recent years [35, 36]. Method for generation of single-cycle squeezed

light by parametric down-conversion, as well as a scheme for observation has been proposed in [37].

While homodyne-detection routines are in principle excellent for selecting a given mode for measurements, during the interaction of attosecond pulses with matter, the collective field plays role. Beyond calculating the quadrature-variance spectrum, but beyond that, we introduce an approximate, single collective noise ellipse. The measurement of the electric field at a spacetime point would require placing (a not completely localizable) test charge at that point. Independently of the technical details of the field measurement, one only can obtain a weighted average of the field over a region [38]. Let us use notation $\Lambda_n \equiv \sqrt{\frac{\hbar\omega_n}{2\epsilon_0 V}}$, and introduce the spatial mean-field operator:

$$\tilde{E}(\vec{r}, t) = \int f(\vec{\rho}) E(\vec{r} - \vec{\rho}, t) d\rho^3 \quad (8)$$

where the $f(\vec{\rho})$ is a real, normalized weighting function. The dimension of $f(\vec{\rho})$ physically corresponds to the spatial extension of the detector (or atom) with which the attosecond pulse interacts. For simplicity, we will assume this function to be only a function of $|\rho|$, then the Fourier-integral becomes: $f(\vec{q}) \equiv \frac{4\pi}{q} \int_0^\infty \rho f(\rho) \sin(q\rho) d\rho$, then:

$$\tilde{E}(\vec{r}, t) = \sum_{q,s} \Lambda_q \left(a_{qs}(t) f(q) e^{i\vec{q}\vec{r}} \bar{\epsilon}_{qs} + a_{qs}^{\dagger}(t) f(q) e^{-i\vec{q}\vec{r}} \bar{\epsilon}_{qs}^* \right). \quad (9)$$

We will only deal with modes propagating in a single direction, with a fixed \vec{r} parameter, and one linear polarization. Then it follows that

$$\tilde{E}(r, t) \approx \sum_q 2\Lambda_q f(q) \left(X_q(t) \cos(qr) + Y_q(t) \sin(qr) \right). \quad (10)$$

from which we define a collective noise-ellipse with its diagonal terms below. For practical purposes we neglect all cross-mode terms (e.g. $\langle a_i a_j^{\dagger} \rangle$) appearing in the evaluation.

$$\langle (\Delta X_{\Sigma})^2 \rangle \equiv \sum_q \Lambda_q f(q) \langle (\Delta X_q)^2 \rangle \quad (11)$$

$$\langle (\Delta Y_{\Sigma})^2 \rangle \equiv \sum_q \Lambda_q f(q) \langle (\Delta Y_q)^2 \rangle \quad (12)$$

We note here, that in relevant calculations we will use gaussian cutoff function. Naturally, these collective quadratures only offer a heuristic insight into the properties of the attosecond pulses.

IV. TIME-EVOLUTION OF QUADRATURE-OPERATORS

In order to calculate time-dependence of the squeezing spectrum, we will implement a system of dynamical equations describing the time-evolution of expectation values. Due to the nonlinearity of the operator-equations, one needs to introduce a hierarchy of equations involving a factorization of expectation values that is physically acceptable. Naturally, choosing the lowest order of factorization, that is, assuming $\langle \sigma_i a_j^{(\dagger)} \rangle \approx \langle \sigma_i \rangle \langle a_j^{(\dagger)} \rangle$ is insufficient for the calculation of quantum properties. In fact this approximation can be considered to be the defining attribute of semiclassical radiation theory [39].

In the following, we will use notation:

$$U = \sigma_x, \quad V = \sigma_y, \quad W = \sigma_z;$$

$$\begin{aligned} U_n^\pm &= (i)^{(1\mp 1)/2} \sigma_x (a_n \pm a_n^\dagger), \\ V_n^\pm &= (i)^{(1\mp 1)/2} \sigma_y (a_n \pm a_n^\dagger), \\ W_n^\pm &= (i)^{(1\mp 1)/2} \sigma_z (a_n \pm a_n^\dagger). \end{aligned}$$

The exact, closed system of dynamical equations, written in terms of these operators can be seen in Appendix A. We will neglect cross-mode correlations and atomic-high order field correlations, implying $\langle a_i^{(\dagger)} a_j^{(\dagger)} \rangle = \langle a_i^{(\dagger)} \rangle \langle a_j^{(\dagger)} \rangle$ if $i \neq j$ and $\langle \sigma_i N_i \rangle = \langle \sigma_i \rangle \langle N_i \rangle$. Numerical investigations imply that these approximations are acceptable [1] as long as the photon number expectation values are reasonably small. Then the dynamical equations are:

$$\begin{aligned} \dot{\langle N_n \rangle} &= \frac{\Omega_n}{2} \langle U_n^- \rangle \\ \dot{\langle U \rangle} &= \omega_0 \langle V \rangle \\ \dot{\langle V \rangle} &= -\omega_0 \langle U \rangle + \Omega(t) \langle W \rangle + \sum_n \Omega_n \langle W_n^+ \rangle \\ \dot{\langle W \rangle} &= -\Omega(t) \langle V \rangle - \sum_n \Omega_n \langle V_n^+ \rangle \\ \dot{\langle U_n^+ \rangle} &= \omega_0 \langle V_n^+ \rangle - \omega_n \langle U_n^- \rangle \\ \dot{\langle U_n^- \rangle} &= \omega_0 \langle V_n^- \rangle + \omega_n \langle U_n^+ \rangle + \Omega_n \\ \dot{\langle V_n^+ \rangle} &= -\omega_0 \langle U_n^+ \rangle - \omega_n \langle V_n^- \rangle + \Omega(t) \langle W_n^+ \rangle \\ &\quad + \Omega_n \langle W \rangle (1 + 2\langle N_n \rangle + 2\langle X_{2n} \rangle) + \sum_{j \neq n} 2\Omega_j \langle W_n^+ \rangle \langle X_j \rangle \\ \dot{\langle V_n^- \rangle} &= -\omega_0 \langle U_n^- \rangle + \omega_n \langle V_n^+ \rangle + \Omega(t) \langle W_n^- \rangle \\ &\quad - 2\Omega_n \langle W \rangle \langle Y_{2n} \rangle - 2 \sum_{j \neq n} \Omega_j \langle W_n^- \rangle \langle X_j \rangle \\ \dot{\langle W_n^+ \rangle} &= -\omega_n \langle W_n^- \rangle - \Omega(t) \langle V_n^+ \rangle \\ &\quad - \Omega_n \langle V \rangle (1 + 2\langle N_n \rangle + 2\langle X_{2n} \rangle) - 2 \sum_{j \neq n} \Omega_j \langle V_n^+ \rangle \langle X_j \rangle \\ \dot{\langle W_n^- \rangle} &= \omega_n \langle W_n^+ \rangle - \Omega(t) \langle V_n^- \rangle + 2\Omega_n \langle V \rangle \langle Y_{2n} \rangle \\ &\quad - 2 \sum_{j \neq n} \Omega_j \langle V_n^- \rangle \langle X_j \rangle \\ \dot{\langle X_n \rangle} &= \omega_n \langle Y_n \rangle \\ \dot{\langle Y_n \rangle} &= -\frac{\Omega_n}{2} \langle U \rangle - \omega_n \langle X_n \rangle \\ \dot{\langle X_{2n} \rangle} &= -\frac{\Omega_n}{2} \langle U_n^+ \rangle + 2\omega_n \langle Y_{2n} \rangle \\ \dot{\langle Y_{2n} \rangle} &= -\frac{\Omega_n}{2} \langle U_n^+ \rangle - 2\omega_n \langle X_{2n} \rangle \end{aligned}$$

In this article, (similarly to [1]) we will consider the mode-structure of the electromagnetic field to be discrete, and its mode-density independent of frequency.

Results for the 11th harmonic can be observed on Fig.(1). We can summarize the dynamics of the (anti)squeezing as: Principal variances (λ_\pm oscillate in time, –with periods that depends only on the frequency of the mode– and within a certain order of magnitude. The results of numerical calculations show that this magnitude follows a non-monotonic dependence on the amplitude of the short pulse, while it grows monotonically with $\Omega/\sqrt{\omega}$.

Within each half-cycle of the excitation (corresponding to individual attosecond pulses within the train) the evolution of quadrature-variances are very close to being periodical.

There are certain time-intervals within of which squeezing occurs. To characterize this, the principal variances do not suffice in themselves, one needs to define appropriate phases for the field. We will only use the most straightforward definition of the phase-operator, specifying its mean value as

$$\phi \equiv \text{atan2}(\langle X \rangle, \langle Y \rangle). \quad (13)$$

Amplitude-; and the associated orthogonal variance can then be written as: $\langle (\Delta X^\phi)^2 \rangle$; $\langle (\Delta Y^\phi)^2 \rangle$.

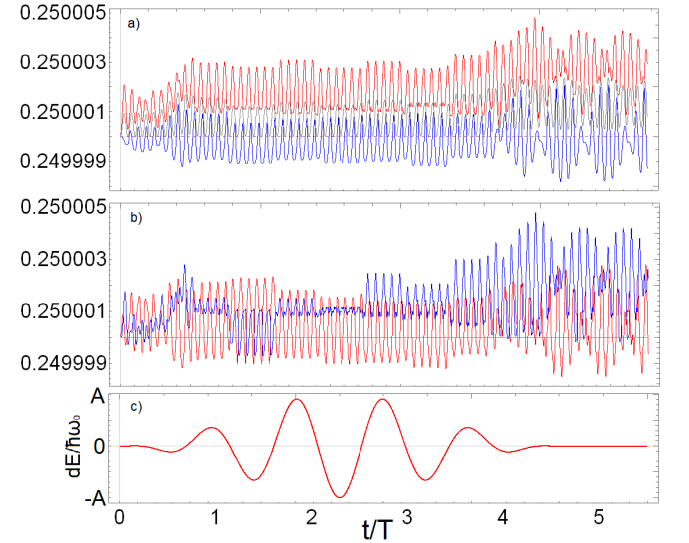


FIG. 1: Quadrature variances of the 11th harmonic. Subfig. a) Time evolution of the maximal λ_+ (red) and minimal λ_- (blue) variances. The geometric mean $\sqrt{\lambda_+ \lambda_-} > 1/4$ is shown in gray. Subfig. b) Time-evolution of $\langle (\Delta X^\phi)^2 \rangle$ (red) and $\langle (\Delta Y^\phi)^2 \rangle$ (blue). Subfig. c) shows the time-dependence of the excitation. The parameters correspond to the A amplitude of the exciting pulse being 100 in the given units, while $\Omega_n/\sqrt{\omega_n} = 0.005$. The excitation is resonant.

Numerical results imply that when squeezing is present in a given mode, then the state is usually close to be-

ing amplitude squeezed. It worth noting that amplitude-squeezing and sub-Poissonian photon statistics are connected, however in photon-counting experiments the sub-poissonian nature would be probably blurred, due to the integration time, as well as due to the relatively limited frequency-selectivity.

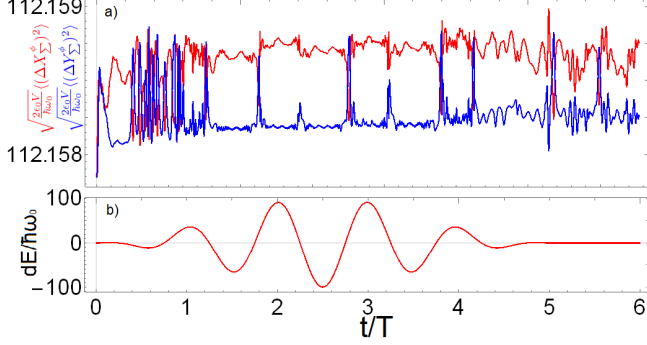


FIG. 2: Subfig. a) Time-evolution of the collective amplitude-variance, and the orthogonal variance. The calculation included 200 modes, evenly distributed between the 5th and 25th harmonic. The regularization was chosen such that the modes above the 22th harmonic give small contribution. Subfig. b) and the parameters are the same as in Fig.(1)

The calculations suggests that the collective quadrature-variances as defined in III A exhibit modest relative oscillations within each pulse. There is no point in time in which the collective variances have lower value then in the initial state, and in contrast with individual modes, the variance of the amplitude is larger then that of the orthogonal coordinate. One can compare sections of the photon-number spectrum with the spectrum of amplitude-(anti)squeezing. The structure and the order of magnitudes are similar. The adiabatically changing characteristics –the tendency of some value to change abruptly in each half-cycle of the excitation– of the quadrature-variance is more significant then that of that of the photon-numbers however. This is due to the fact that quadratures are directly driven by the value of $\langle U \rangle$, which itself is strongly adiabatical.

We hypothesize that the attosecond-pulse trains emitted by certain realistic solid-state targets (with similar dipole-evolution) follows at least some of the characteristics we have described.

V. CONCLUSIONS

We have given a set of equations, with which the time-evolution of photon numbers as well as quadrature-amplitudes and variances can be followed simultaneously. Quadrature variances of each separate mode oscillate with frequency that depends only on the mode, and amplitude that is largely constant within each generated pulse. This latter property is similar to the adiabatically changing mean dipole-operator.

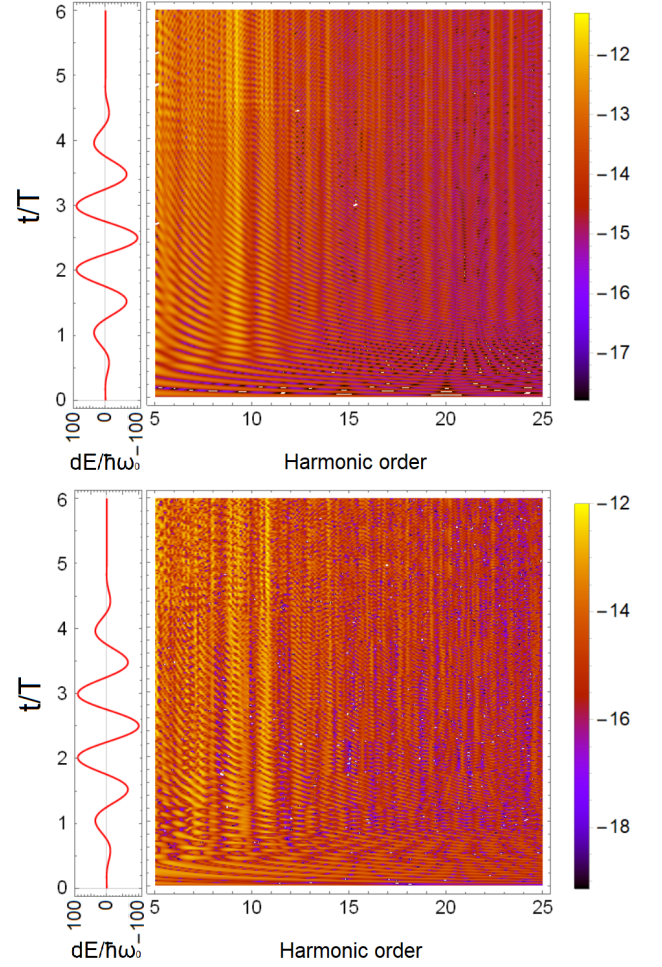


FIG. 3: Top: Time-evolution of photon numbers on logarithmic scale. Bottom: Time-evolution of the absolute difference of the amplitude-variance from $1/4$, on logarithmic scale.

The different quadrature-variances can be additional information for the characterization of high harmonics and of attosecond pulses. Our calculations also suggest a weak, nearly-amplitude squeezing in individual high harmonics, which may be of metrological use.

Appendix A: Exact operator-equations

A system of exact dynamical operator-equations guiding the time-evolution of the multi-mode Rabi-model with an added time-dependent classical excitation is given below.

$$\begin{aligned}\dot{N}_n &= \frac{\Omega_n}{2} U_n^- \\ \dot{U} &= \omega_0 V \\ \dot{V} &= -\omega_0 U + \Omega(t) W + \sum_n \Omega_n W_n^+ \\ \dot{W} &= -\Omega(t) V - \sum_n \Omega_n V_n^+ \\ \dot{U}_n^+ &= \omega_0 V_n^+ - \omega_n U_n^- \\ \dot{U}_n^- &= \omega_0 V_n^- + \omega_n U_n^+ + \Omega_n\end{aligned}$$

$$\begin{aligned}
\dot{V}_n^+ &= -\omega_0 U_n^+ - \omega_n V_n^- + \Omega(t) W_n^+ + \sum_j \Omega_j W_n^+ (a_j + a_j^\dagger) \\
\dot{W}_n^+ &= -\omega_n W_n^- - \Omega(t) V_n^+ - \sum_j \Omega_j V_n^+ (a_j + a_j^\dagger) \\
\dot{V}_n^- &= -\omega_0 U_n^- + \omega_n V_n^+ + \Omega(t) W_n^- + \Omega_n W_i (a_n^2 - a_n^{\dagger 2}) - \sum_{j \neq n} \Omega_j W_j^+ i(a_n^\dagger - a_n) \\
\dot{W}_n^- &= \omega_n W_n^+ - \Omega(t) V_n^- - \Omega_n V_i (a_n^2 - a_n^{\dagger 2}) + \sum_{j \neq n} \Omega_j V_j^+ i(a_n^\dagger - a_n) \\
(a_n^\dagger + a_n) &= \omega_n i(a_n^\dagger - a_n) \\
i(a_n^\dagger - a_n) &= -\Omega_n U - \omega_n (a_n^\dagger + a_n) \\
i(a_n^{\dagger 2} - a_n^2) &= -\Omega_n U_n^+ - 2\omega_n (a_n^{\dagger 2} + a_n^2) \\
(a_n^{\dagger 2} + a_n^2) &= -\Omega_n U_n^- + 2\omega_n i(a_n^{\dagger 2} - a_n^2)
\end{aligned}$$

Appendix B: Excitation induced nonlinearity

Due to the nonlinearity of the dynamics, squeezing is guaranteed, but dependencies on time, the excitation, and material properties are nontrivial. Here we present a qualitative result for the case of weak coupling $\Omega_n \ll 1$ and not too strong excitation, such that $\Omega_n^2 \Omega(t) \lesssim 1$. Let us note that in certain cases an operational measure [29] of squeezing is used, based on the separation of the Hamiltonian as:

$H(t) = H_{\text{passive}}(t) + \sum_j c_j(t) H_{\text{squeeze}_j}(t)$; after which the amount of squeezing is measured as

$$f_{sq}(t) = \int_0^t \sum_j |c_j(\tau)| d\tau. \quad (\text{B1})$$

It is not immediately obvious how one should separate H_{qc} into non-squeezing and squeezing terms. One way to proceed is to recast the Hamiltonian into a form where the counter-rotating terms in H_{am} vanish. In the absence of $H_{ex}(t)$, photon numbers would then be conserved up to the order of $\frac{\Omega_n}{2(\omega_0 + \omega_n)}$, and an infinite series of terms corresponding to higher-photon processes appear. However, due to the classical excitation, new counterrotating terms will be present, and can become dominant in the strong-field limit. With the assumptions above, the lead-

ing terms we may associate with squeezing are of the form:

$$\frac{\hbar \Omega_n^2}{4(\omega_0 + \omega_n)} \left[\sigma_z (a_n^{\dagger 2} + a_n^2) - \frac{\Omega(t)}{8(\omega_0 + \omega_n)} (\sigma_- a_n^2 + \sigma_+ a_n^{\dagger 2}) \right] + o(\Omega_n^3 \Omega(t)). \quad (\text{B2})$$

This could lead us to the qualitative conclusion that –up to first-order perturbation– (anti)squeezing increases roughly quadratically with Ω_n^2 and linearly field-amplitude. Numerical calculations show that this conclusion is only acceptable in very limited regime of parameters however, and should not be considered quantitatively indicative.

Appendix C: Extraction of the nonlinear term

Let us define the following operator [40]:

$$V = \exp \left(\underbrace{\epsilon (a_i^\dagger \sigma_+ + a_i \sigma_-)}_A \right) \quad (\text{C1})$$

where ϵ is small.

Then $V H V^\dagger \approx H + [A, H] + \frac{1}{2} [A, [A, H]]$ Using the notation $\bar{\omega} = \frac{\omega_0 + \omega_j}{2}$ we can write:

$$\begin{aligned}
V H V^\dagger &\approx H + \epsilon [(a_i^\dagger \sigma_+ - a_i \sigma_-), H] \\
&\quad + \frac{\epsilon^2}{2} [a_i^\dagger \sigma_+ - a_i \sigma_-, [a_i^\dagger \sigma_+ - a_i \sigma_-, H]] \\
&= H - 2\epsilon \hbar \bar{\omega} (\sigma_+ a^\dagger + \sigma_- a) - \epsilon^2 \hbar \bar{\omega} (\sigma_z (2N + 1) - 1) \\
&\quad + \epsilon \frac{\hbar \Omega_n}{2} \sigma_z (a^{\dagger 2} + a^2) - \epsilon^2 \frac{\hbar \Omega_n}{2} (\sigma_+ a^{\dagger 3} + \sigma_- a^3 + \sigma_+ a N + \sigma_- N a^\dagger) \\
&\quad + \epsilon \frac{\hbar \Omega_n}{2} (\sigma_z (2N + 1) - 1) - 2\epsilon^2 \frac{\hbar \Omega_n}{2} (\sigma_- a N + \sigma_+ N a^\dagger) \\
&\quad + \epsilon \frac{\hbar \Omega(t)}{2} \sigma_z (a^\dagger + a) - \epsilon^2 \frac{\hbar \Omega(t)}{4} (2\sigma_- a^2 + 2\sigma_+ a^{\dagger 2} + 2N \sigma_x + \sigma_x).
\end{aligned}$$

It is customary to choose $\epsilon = \frac{\Omega_n}{4\bar{\omega}}$, so that the counter-rotating term in H disappears. Then the transformed Hamiltonian conserves the photon number up to ϵ . However, if the excitation is strong, the counterrotating term proportional with $\epsilon^2 \Omega(t) \ll 1$ becomes dominant, introducing nonlinearity.

-
- [1] Ákos Gombkötő, A. Czirják, S. Varrò, and P. Földi, *Phys. Rev. A* **94**, 013853 (2016).
 - [2] L. V. Keldysh, *Sov. Phys. JETP* **20**, 1307 (1964).
 - [3] F. Krausz and M. Ivanov, *Rev. Mod. Phys.* **81**, 163 (2009).
 - [4] M. Lewenstein, P. Balcou, M. Y. Ivanov, A. L’Huillier, and P. B. Corkum, *Phys. Rev. A* **49**, 2117 (1994).
 - [5] G. Farkas and C. Tóth, *Phys. Lett. A* **168**, 447 (1992).
 - [6] M. Ferray, A. L’Huillier, X. F. Li, L. A. Lompre, G. Mainfray, and C. Manus, *J. Physics B* **21**, L31 (1988).
 - [7] P.-L. He, C. Ruiz, and F. He, *Phys. Rev. Lett.* **116** (2016).
 - [8] M. Garg, M. Zhan, T. T. Luu, H. Lakhota, T. Klostermann, A. Guggenmos, and E. Goulielmakis, *Nature* **538**, 359 (2016).
 - [9] C. Guo, A. Harth, S. Carlström, Y.-C. Cheng, S. Mikaelsson, E. Morsell, C. Heyl, M. Miranda, M. Gisselbrecht, M. Gaarde, et al., *J. Phys. B* **51** (2017).
 - [10] J. Xu, B. Shen, X. Zhang, Y. Shi, L. Ji, L. Zhang, T. Xu, W. Wang, X. Zhao, and Z. Xu, *Sci. Rep.* **8** (2018).
 - [11] M. Kizmann, T. Guedes, D. Seletskiy, A. Moskalenko, A. Leitenstorfer, and G. Burkard, *Subcycle squeezing of light from a time flow perspective* (2019).
 - [12] T. Iskhakov, M. Chekhova, and G. Leuchs, *Phys. Rev. Lett.* **102**, 183602 (2009).
 - [13] M. Xiao, L.-A. Wu, and H. Kimble, *Phys. Rev. Lett.* **59**, 278 (1987).
 - [14] E. Polzik, J. Carri, and H. Kimble, *Phys. Rev. Lett.* **68**, 3020 (1992).
 - [15] R. Boyd, S. Lukishova, and V. Zadkov, *Quantum Pho-*

- tonics: Pioneering Advances and Emerging Applications (Springer Series in Optical Sciences 217)* (2019), ISBN 978-3-319-98402-5.
- [16] J. Gea-Banacloche, Phys. rev. lett. **62**, 1603 (1989).
 - [17] W. P. B. C. F. H.-A. B. P. K. L. Nicolas Treps, Nicolas Grosse, Science **301**, 940 (2003).
 - [18] M. Rosenbluh and R. Shelby, Phys. Rev. Lett. **66**, 153 (1991).
 - [19] U. S. A. S. S. Splter, M. Burk and G. Leuchs, Opt. Express **2**, 77 (1998).
 - [20] C. Riek, P. Sulzer, M. Seeger, A. S. Moskalenko, G. Burkard, D. V. Seletskiy, and A. Leitenstorfer, Nature **541**, 376379 (2017).
 - [21] W. Wasilewski, A. Lvovsky, K. Banaszek, and C. Radzewicz, Phy. Rev. A **73** (2006).
 - [22] kos Gombkt, P. Foldi, and S. Varr (in preparation).
 - [23] J. N. Heyman, K. Craig, B. Galdrikian, M. S. Sherwin, K. Campman, P. F. Hopkins, S. Fafard, and A. C. Gosard, Phys. Rev. Lett. **72**, 2183 (1994).
 - [24] Y. Zhan, Proc. SPIE (1992).
 - [25] D. F. Walls and G. J. Milburn, *Quantum Optics* (Springer-Verlag, Berlin, 1994).
 - [26] M. Collett and D. Walls, Phys. Rev. A **32** (1985).
 - [27] J. Peina, *Quantum Statistics of Linear and Nonlinear Optical Phenomena* (1991).
 - [28] A. Luk, V. Peinov, and J. Peina, Opt. Commun. **67**, 149151 (1988).
 - [29] M. Idel, D. Lercher, and M. Wolf, Journal of Physics A: Mathematical and Theoretical **49** (2016).
 - [30] C. Lee, Optics Communications **66**, 52 (1988).
 - [31] G. Breitenbach, F. Illuminati, S. Schiller, and J. Mlynek, EPL **44**, 192 (2007).
 - [32] Y. Shaked, Y. Michael, R. Vered, L. Bello, M. Rosenbluh, and A. Pe'er, Nat. Commun. **9** (2018).
 - [33] R. Schnabel, Phys. Rep. **684** (2016).
 - [34] H. Kimble, Y. Levin, A. Matsko, K. Thorne, and S. Vatchanim, Phys. Rev. D **65** (2002).
 - [35] E. Oelker, G. Mansell, M. Tse, J. Miller, F. Matichard, L. Barsotti, P. Fritschel, D. McClelland, M. Evans, and N. Mavalvala, Optica **3**, 682 (2016).
 - [36] N. Straniero, J. Degallaix, R. Flaminio, L. Pinard, and G. Cagnoli, Opt. Express **23**, 21455 (2015).
 - [37] V. Z. Reinier W. Heeres, Leo P. Kouwenhoven, Nat Nanotechnol. 2013 Oct;8(10):719-22 **8**, 719722 (2013).
 - [38] O. Keller, *Quantum Theory of Near-Field Electrodynamics* (2011), ISBN 978-3-642-17409-4.
 - [39] L. Allen and J. H. Eberly, *Optical resonance and two-level atoms*, Dover books on physics (Dover, New York, NY, 1987).
 - [40] A. B. Klimov and S. Chumakov, *A group-theoretical approach to quantum optics : models of atom-field interactions* (2009).